FINAL REPORT GRANT NO. ER46517

Anisometric C_{60} Fullerene Colloids Assisted by Structure-Directing Agent

S. Penterman and C. M. Liddell Watson

Crystal Engineering Communications, 18 (2016): 1775-1781 DOI: 10.1039/c5ce02122g

Colloidal synthesis and assembly provide low cost, large area routes to mesoscale structures. In particular, shape-anisotropic particles may form crystalline, plastic crystalline, complex liquid crystalline and glassy phases. Arrangements in each order class have been used to generate photonic materials. For example, large photonic band gaps have been found for photonic crystals,[1] hyperuniform photonic glasses,[2] and also for plastic crystals[3] at sufficient refractive index contrast. The latter structures support highly isotropic bandgaps that are desirable for free-form waveguides and LED out-coupling.[4] Photonic glasses with optical gain lead to self-tuned lasing by the superposition of multiply scattered light.[5] Typically, extrinsic media such as organic dyes, rare earths, lanthanides and quantum dots are used to impart optical gain in photonic solids.[6-8]

The present work advances fullerene microcrystals as a new materials platform for 'active' light emitting in colloid-based photonic crystals. Fullerenes support singlet excited states that recombine to produce a characteristic red photoluminescence. C_{60} also has a high refractive index ($n \sim 2.2$) and transparency (> 560 nm)[9] so that inverse structures are not required.

Co-solvent precipitation (or solvent-antisolvent precipitation) promotes dynamic controls in the synthesis of fullerene microcrystals. Fullerene solutions are emulsified in a poor solvent and diffusion of the good solvent leads to supersaturation and nucleation. The solvent properties including molecular shape, fullerene solubility, viscosity and miscibility are critical in determining the colloidal morphology.[10-12] In suitable systems, the solvent-antisolvent ratio, fullerene concentration and mixing conditions can be tuned to obtain uniform colloids with diverse forms. However, solvent-antisolvent compatibility is nontrivial and only a few combinations have been utilized for the synthesis of monodisperse colloids.

We synthesized C_{60} solvated microcrystals via co-solvent precipitation with a nitrogen moiety in the good solvent. The nitrogen moiety associates with the faces of the growing crystal because of its amphiphilicity. This stabilizes crystal growth in solvent systems with potential for producing monodisperse particles in greater quantity. Specifically, fullerene microcrystals were prepared from 1,2,3,4-tetrahydronaphthalene (THN) or mesitylene in 2-propanol antisolvent using 20% v/v 2,4,6-trimethylpyridine (TMP) as the surface active agent. The primary solvents enable working with higher fullerene concentrations, but the growth is uncontrolled in the absence of TMP and irregular aggregates are obtained. A schematic of co-solvent precipitation assisted by a structure-directing agent is depicted in Fig. 1. Diverse morphologies including well-faceted rod shapes with coefficient of variation (CV) < 4% are obtained as a function of solvent-antisolvent ratio and fullerene

concentration (Fig. 2). Time-resolved fluorescence spectroscopy and confocal fluorescence image analysis indicated microcrystals made with the mixed solvent system (THN/TMP) had a reduced fluorescence quantum yield and lifetime. These results may be attributed to exciton–exciton annihilation interactions, which increase with greater fullerene packing efficiency. Our results suggest that packing efficiency and monodispersity of the microparticles are enhanced because the polar additive acts as a blocking agent and slows growth on specific crystal facets. Additionally, the polar structure directing agent shortens the nucleation period and enhances the monodispersity of the fullerene colloids.

References

1 G. von Freymann, V. Kitaev, B. V. Lotsch and G. A. Ozin, *Chem. Soc. Rev.*, 2013, **42**, 2528.

2 W. Man, M. Florescu, K. Matsuyama, P. Yadak, G. Nahal, S. Hashemizad, E. Williamson, P. Steinhardt, S. Torquato and P. Chaikin, *Opt. Express*, 2013, **21(17)**, 19972.

3 A. C. Stelson, C. Avendano and C. M. Liddell Watson. *J. Appl. Phys.*, 2016, **119,** 023110.

4 M. Hejna, Ph.D. Thesis, Princeton University, 2013.

5 J. F. Galisteo-López, M. Ibisate, R. Sapienza, L. S. Froufe-Pérez, A. Blanco and C. López, *Adv. Mater.*, 2011, **23**, 30.

6 J. Kalkman, E. de Bres, A. Polman, Y. Jun, D. J. Norris, D. C. 't Hart, J. P. Hoogenboom and A. van Blaaderen, *J. Appl. Phys.*, 2004, **95**, 2297.

7 A. Yadav, R. De Angelis, M. Casalboni, F. De Matteis, P. Prosposito, F. Nanni and I Cacciotti, *Opt. Mater.*, 2013, **35**, 1538.

8 S. Gupta and E. Waks, *Opt. Express*, 2013, **21(24)**, 29612.

9 V. Capozzi, G. Casamassima, G. F. Lorusso, A. Minafra, R. Piccolo, T. Trovato and A. Valentini, *Sol. State Comm.*, 1996, **98(9)**, 853.

10 J. Jeong, W. Kim, S. Park, T. Yoon and B. H. Chung, *J. Phys. Chem. C*, 2010, **114**, 12976.

11 H. Ji, J. Hu, Q. Tang, W. Song, C. Wang, W. Hu, L. Wan and S. Lee, *J. Phys. Chem C*, 2007, **111**, 10498.

12 A. Masuhara, Z. Tan, H. Kasai, H. Nakanishi and H. Oikawa, *Jap. J. Appl. Phys.*, 2009, **48**, 050206.

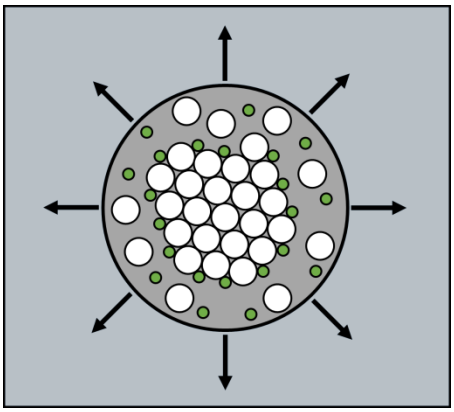

Fig. 1. Schematic growth of fullerene crystals in solvent mixtures in the presence of a structure-directing agent. Solutions of C_{60} (white) in good solvent mixtures (grey) are dispersed in antisolvent (blue). Droplet shrinkage due to solvent interdiffusion induces nucleation. The structure-directing agent (green) shortens the nucleation period and associates with the interface, slowing growth.

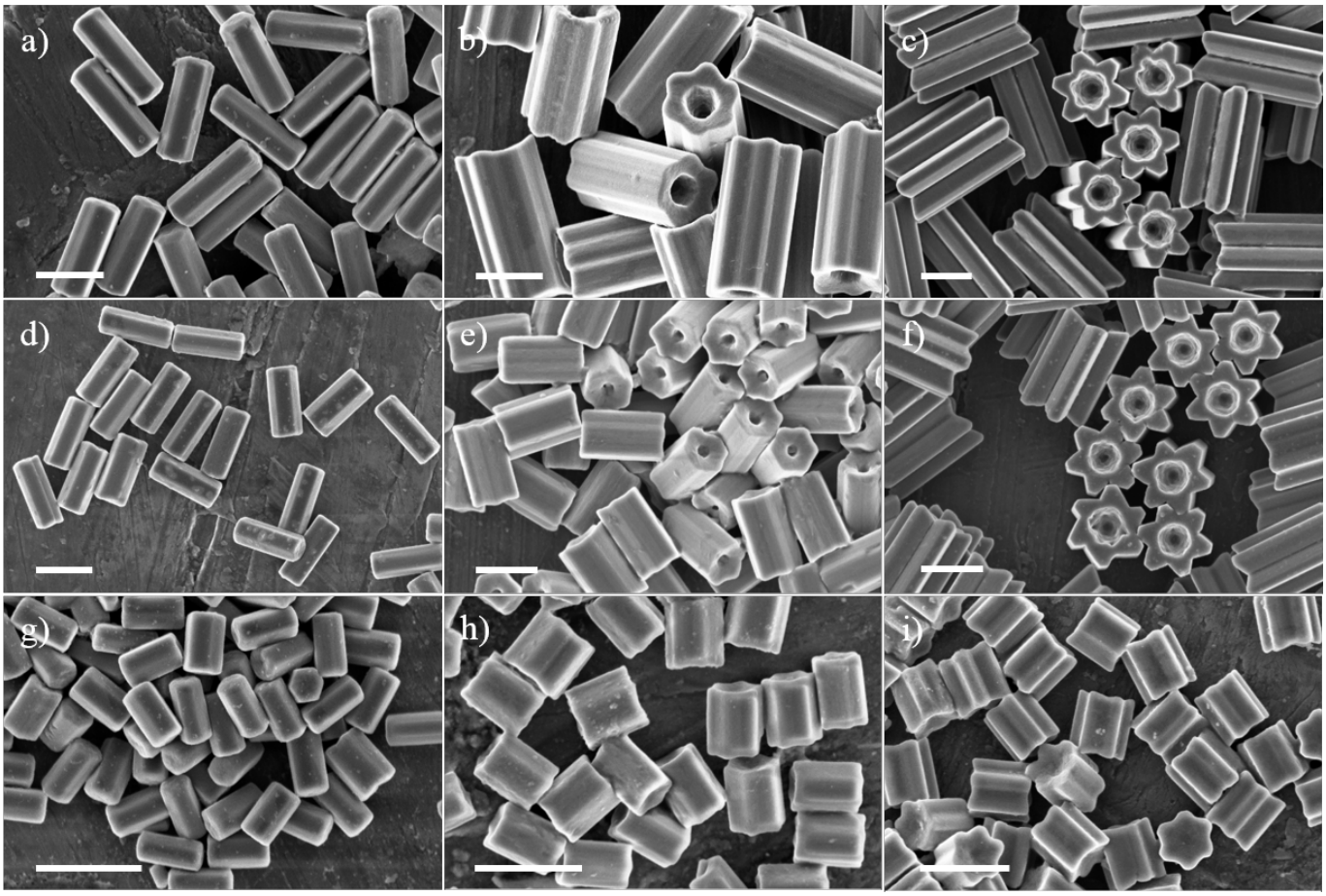

Fig. 2. SEM images of C_{60} solvates prepared in 80:20 tetralin/TMP mixed solvent as a function of fullerene concentration and injection volume. a) 1.6 mM, 150 µL; b) 1.6 mM, 300 µL; c) 1.6 mM, 450 µL; d) 1.8 mM, 150 µL; e) 1.8 mM, 300 µL; f) 1.8 mM, 450 µL; g) 2 mM, 150 µL; h) 2 mM, 300 µL; i) 2 mM, 450 µL. Scale bars represent 1 µm.

Student Support

Sonny Penterman was fully supported in SP 2016 and partially supported in FA 2015 (3 months) on this grant.

Acknowledgments

"This work was supported by the U.S. Department of Energy, Office of Basic Energy Sciences, Division of Materials Sciences and Engineering under award Grant No. ER46517. The facilities used in this work were funded by NSF under agreements DMR-0520404 and DMR-1120296, as well as ECS-0335765 and ECS-9876771."

Phase Behavior of Polyhedral Nanoparticles in Parallel Confinement

M. Khadilkar and F. A. Escobedo

Soft Matter 12, 2016: 1506-1516 DOI:10.1039/c5sm02570b

Monte Carlo simulations were used to investigate the phase behavior of hard cubes, truncated cubes, cuboctahedra and truncated octahedra when confined between two parallel hard walls. The walls are separated by a distance H* (in units of particle in-diameter) which is varied to accommodate a different number of layers, from a monolayer up to approximately 5 layers, hence allowing us to probe the transitional phase behavior as the system goes from a quasi-2D geometry to a quasi-3D bulk behavior. While our results do reveal some phases whose structures resemble those that have been observed before for such systems in 2D and 3D spaces, other phases are also detected, including buckled phases, rotator plastic phases, and solids with significant translational disorder. Ordered phases formed for H* values that are a little too narrow to accommodate an additional particle layer are particularly interesting as they tend to have complex structures. Figure 3 shows sample results of truncate octahedral (TO). The maximum density for such frustrated phases is low compared to that of non-frustrated ones for the same system at different H*. As the asphericity in the shapes is reduced, the simulated phases show structural features that approach those of the phases that have been reported for hard spheres under similar confinement.

Student Support

M. Khadilkar was fully supported by DOE Grant for one Semester in 2015.

Acknowledgments

"Funding support is gratefully acknowledged from DOE (Office of Basic Energy Sciences, Division of Materials Sciences and Engineering under award Grant No. ER46517). The authors also thank Dr U. Agarwal and V. Thapar for useful exchanges."

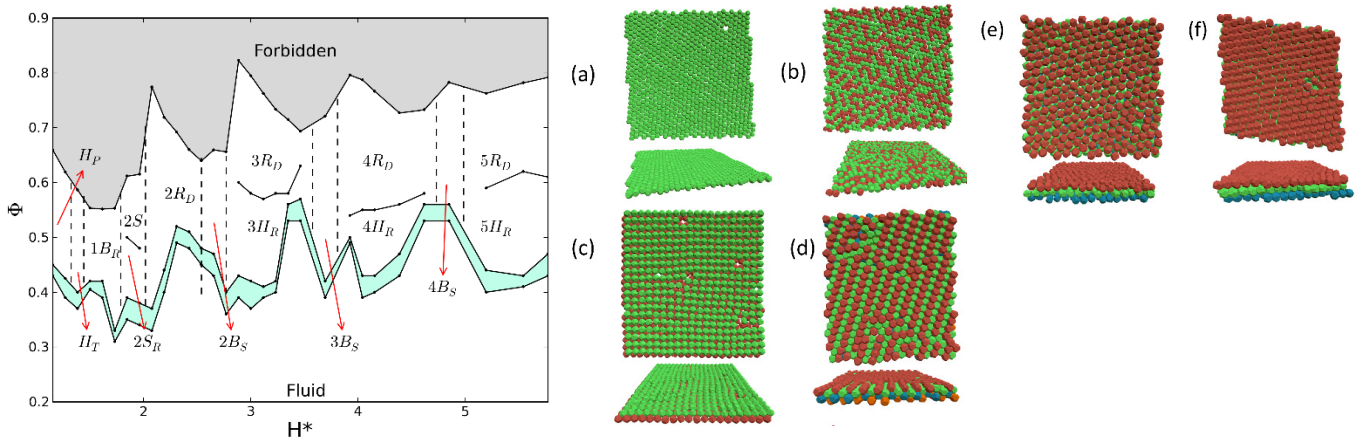

Fig. 3. Truncated octahedral in slit confinement. **Top:** Volume fraction Φ vs. confinement H* phase diagram. Green shaded areas represent two-phase coexistence regions, gray regions are inaccessible, & vertical dashed lines give approximate phase boundaries. **Right:** Snapshots (top and side view) of phases at representative confinements: (a) Hexagonal parallel (H_P), H*=1.2 and Φ ≈ 0.53; (b) Buckled rhombic ($1B_R$), H* = 1.6 and Φ ≈0.56; (c) 2-layer rotator square ($2S_R$) phase, H* = 1.9 and Φ ≈0.66; (d) 2-layer buckled square ($2B_S$), H*= 2.8 and Φ ≈0.67; (e) 3-layer hexagonal rotator ($3H_R$), H*= 3.3 and Φ ≈0.51; (f) 3-layer distorted rhombic ($3R_D$), H*= 3.3 and Φ ≈0.64.

Assembly of Highly Open Smectic Structures Formed From Interlocking High-Symmetry Planar Nanorings

C. Avendaño, G. Jackson, E. A. Müller, and F. A. Escobedo

In press *Proc. Natl. Acad. Sci.*, USA (2016)

Materials comprising porous structures, often in the form of interconnected concave cavities, are typically assembled from convex molecular building blocks. The use of nanoparticles with a characteristic nonconvex shape provides a promising strategy to create new porous materials. Nonconvex mesogenic building blocks can be engineered to form unique self-assembled open structures with tunable porosity and long-range order that is intermediate between that of isotropic liquids and of crystalline solids. Here highly open liquid-crystalline structures are designed from rigid nanorings with ellipsoidal and polygonal geometry. By exploiting the entropic ordering characteristics of athermal colloidal particles, it is found that high-symmetry nonconvex rings with large internal cavities interlock within a 2D layered structure leading to the formation of distinctive liquid-crystalline smectic phases. Figure 4 shows some of these phases. We find that these novel smectic phases possess uniquely high free volumes of up to ~95%, a value significantly larger than the 50% that is typically achievable with smectic phases formed by more conventional convex rod- or disklike mesogenic particles. These highly porous structures are unique candidates as adsorption and storage materials due to both their large void volumes and fluidity.

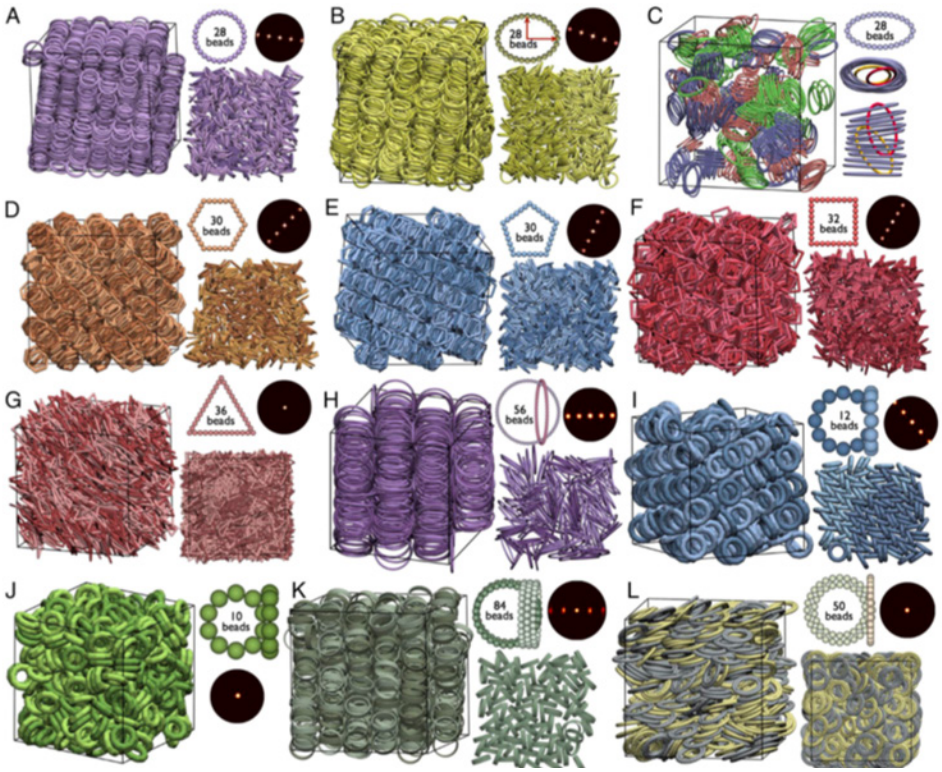

Fig. 4. Particle models and stable microstructures observed in colloidal nanorings of various geometry. A–G show the structures exhibited by rings of different symmetry but with a similar planar area: (A) smectic-A (SmA) phase for circular rings; (B) SmA phase for ellipsoidal rings with an aspect ratio of e=0.85; (C) disordered phase for ellipsoidal rings with e=0.5 exhibiting clustered domains of tubular morphology; (D) and (E) SmA phases for hexagonal and pentagonal rings, respectively; (F) SmA phase for square rings; and (G) nematic (N) phase for triangular rings. In each case we present a single particle with the corresponding number of beads, a snapshot of the liquid-crystalline structure, and a single layer of the SmA phase or an N phase observed along the director. H–J correspond to the phases observed in doughnut-like circular rings of increasing thickness. Systems H and I form SmA phases while system J, having no ring-ring interpenetration, is isotropic. K corresponds to the SmA phase formed by multistacked cylindrical band-like rings comprising three layers. L is the N phase formed by circular washer-like rings comprising one inner layer. In H–L two particles are depicted to visualize the maximum possible interpenetration. The static structure factor projected in a plane containing the director of the system is shown for all systems.

Student Support

No student was directly supported by this Grant, but C. Avendano and F.A. Escobedo started this collaboration when Avendano was a post doc in Escobedo's group and partially supported by DOE Grant.

Acknowledgments

C.A. thanks A. Patti (University of Manchester) for helpful discussions. G.J. and E.A.M. acknowledge funding from the Engineering and Physical Sciences Research Council (Grants EP/E016340, EP/L020564, EP/J010502, and EP/ J014958), and F.A.E. acknowledges funding from the US Department of Energy, Office of Basic Energy Sciences, Division of Materials Sciences and Engineering (Grant ER46517) and the National Science Foundation (Award CBET-1402117).

The Effect of Shear Flow on the Rotational Diffusion of a Single Axisymmetric Particle

Brian D. Leahy, Donald L. Koch, and Itai Cohen

Journal of Fluid Mechanics, 772, 2015: 42-79 DOI:10.1017/jfm.2015.186

Understanding the orientation dynamics of anisotropic colloidal particles is important for suspension rheology and particle self-assembly. However, even for the simplest case of dilute suspensions in shear flow, the orientation dynamics of non-spherical Brownian particles are poorly understood. In this paper we analytically calculate the time dependent orientation distributions for non-spherical axisymmetric particles confined to rotate in the flow–gradient plane, in the limit of small but non-zero Brownian diffusivity. For continuous shear, despite the complicated dynamics arising from the particle rotations, we find a coordinate change that maps the orientation dynamics to a diffusion equation with a remarkably simple ratio of the enhanced rotary diffusivity to the zero shear diffusion: D^r_{eff}/D^r_0 3/8 $(p\text{-}1/p)^2$ + 1, where p is the particle aspect ratio. For oscillatory shear, the enhanced diffusion becomes orientation dependent and drastically alters the long-time orientation distributions. We describe a general method for solving the time-dependent

oscillatory shear distributions (Fig. 5) and finding the effective diffusion constant. As an illustration, we use this method to solve for the diffusion and distributions in the case of triangle-wave oscillatory shear and find that they depend strongly on the strain amplitude and particle aspect ratio. These results provide new insight into the time-dependent orientation and rheology of suspensions of anisotropic particles.

The ability to control the orientation of anisotropic particles opens the door to the development of time dependent flow methods for self-assembly in suspensions comprised of such particles. In particular we are now devising methods for imposing shear protocols that are both uniaxial and biaxial to create flow patterns that can control both the orientation and density of these particles. This new capability is being written up as an additional manuscript.

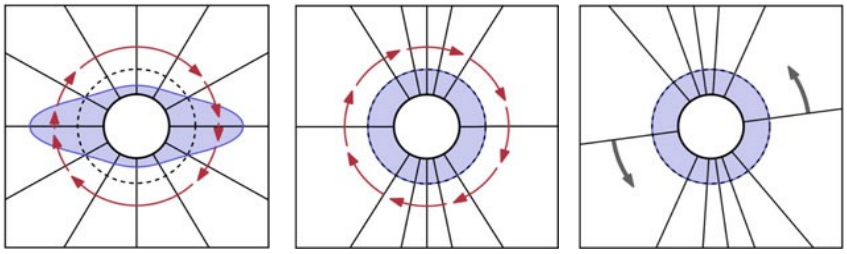

Fig. 5. The continuous-shear distributions $\rho(\varphi)$ for a particle with aspect ratio $p \approx 2.83$. (*a*) $\rho(\varphi)$ in steady state. Here the value of ρ is shown by the distance from the central black ring; the dotted black line shows the zero-shear equilibrium distribution ($\rho = 1/2\pi$). The solid black lines correspond to 12 equally-spaced angles at $\varphi = n\pi/6$. The red arrows indicate the Jeffery orbit velocity. (*b*,*c*) The ancillary distribution f in the stretched space. The angular portion of (2.3), shown in (*b*), stretches the space significantly, visible from the bunched φ gridlines and turns the Jeffery orbit into a uniform rotation. By transforming to a rotating reference frame (*c*), the uniform rotation in (*b*) is removed.

Student Support

Brian Leahy and Neil Lin were supported on this award for 4 and 3 months, respectively.

Acknowledgments

We acknowledge support from the National Science Foundation (CBET-1435013) (D.L.K.), from the US Department of Energy, Office of Basic Energy Sciences, Division of Materials Science and Engineering under Award No. ER46517 (I.C.), and from National Defense Science and Engineering Graduate (NDSEG) Fellowship 32CFR168a (B.D.L.).